



ELSEVIER

Journal of Chromatography A, 694 (1995) 209–218

JOURNAL OF  
CHROMATOGRAPHY A

## Direct determination of E2020 enantiomers in plasma by liquid chromatography–mass spectrometry and column-switching techniques

Kenji Matsui<sup>a,\*</sup>, Yoshiya Oda<sup>b</sup>, Hiroshi Ohe<sup>b</sup>, Shigeru Tanaka<sup>a</sup>, Naoki Asakawa<sup>b</sup>

<sup>a</sup>Department of Drug Metabolism and Pharmacokinetics, Tsukuba Research Laboratories, Eisai Co., Ltd.,  
1–3 Tokodai 5-chome, Tsukuba-shi, Ibaraki 300-26, Japan

<sup>b</sup>Department of Physical and Analytical Chemistry, Tsukuba Research Laboratories, Eisai Co., Ltd., 1–3 Tokodai 5-chome,  
Tsukuba-shi, Ibaraki 300-26, Japan

### Abstract

High-performance liquid chromatography with column switching and mass spectrometry (MS) was applied to the on-line determination and resolution of the enantiomers of E2020 (acetylcholinesterase inhibitor) in plasma. This system employs two avidin columns and fast atom bombardment (FAB)-MS. A plasma sample was injected directly into an avidin trapping column (10 mm × 4.0 mm I.D.). The plasma protein was washed out from the trapping column immediately while E2020 was retained. After the column-switching procedure, E2020 was separated enantioselectively in an avidin analytical column. The separated E2020 enantiomers were specifically detected by FAB-MS without interference from metabolites of E2020 and plasma constituents. The limit of quantification for each enantiomer of E2020 in plasma was 1.0 ng/ml and the intra- and inter-assay relative standard deviations for the method were less than 5.2%. The assay was validated for enantioselective pharmacokinetic studies in the dog.

### 1. Introduction

E2020 is a novel inhibitor of acetylcholinesterase being developed for the treatment of the symptoms of Alzheimer's disease [1]. E2020, the hydrochloride salt of (*R,S*)-1-benzyl-4-[(5,6-dimethoxy-1-indanon)-2-yl]methylpiperidine, is a racemic mixture due to the presence of an asymmetric carbon atom. The enantiomer ratio (*R:S*) is 1:1.

It is necessary to clarify the pharmacokinetic profiles of the individual isomers in a drug development programme [2]. Because E2020 enantiomers interconvert in aqueous solutions

and plasma via a ketoenol intermediate, the rates of racemization for both the (*R*)- and (*S*)-E2020 were the same and the half-life of racemization was about 77.7 h at 37°C, the determination of each enantiomer by LC with a clean-up procedure is very difficult. A rapid and accurate quantitative method without any clean-up procedure such as deproteination, was developed using column-switching techniques [3–7]. The plasma samples were injected directly into the trapping column, which was an avidin column of 10 mm × 4.0 mm I.D. [8,9], without any pre-treatment. Plasma proteins and other hydrophilic constituents were washed out, the valve was then switched and E2020, which was retained on the trapping column, was transferred to an analytical

\* Corresponding author.

avidin column (150 mm × 1.5 mm I.D.), where E2020 enantiomers were optically resolved. Further, owing to the detection of E2020 enantiomers using fast atom bombardment mass spectrometry (FAB-MS) [10], which is suitable for the ionization of polar, non-volatile and thermally labile compounds, E2020 could be detected specifically without interference from metabolites of E2020 and plasma constituents. Moreover, the use of a deuterium-labelled internal standard (E2020-d<sub>7</sub>) markedly improved the reproducibility for the quantification and the wide linear range of the assay is useful for the monitoring of E2020 enantiomers in plasma. When this LC-MS system is used, the sample work-up can be minimized and the risk of artificial interconversion of E2020 enantiomers is reduced.

This method was applied to the simultaneous determination of the enantiomers of E2020 in dog plasma. There was no difference in the pharmacokinetic profiles of the individual isomers and the *in vivo* interconversion of E2020 enantiomers was slow.

## 2. Experimental

### 2.1. Chemicals

E2020, which is a racemic mixture and a hydrochloride salt, was synthesized at Eisai. Each enantiomer [(*R*)- and (*S*)-E2020] was isolated from racemic E2020 by HPLC as the free base. Its plausible metabolites and E2020-d<sub>7</sub>, were synthesized at Eisai. Structures are shown in Fig. 1. Other reagents and solvents were of analytical-reagent or LC grade (Wako, Osaka, Japan).

### 2.2. Apparatus

The LC system consisted of an SCL-10A system controller, an LC10AD pump, an SIL-10A autosampler and an FCV-12AH switching valve (Simadzu, Kyoto, Japan). In this system, a 5- $\mu$ m Biopstick AV-1 column of 10 mm × 4.0 mm I.D. (GL Sciences, Tokyo, Japan) as a trapping column was eluted with 50 mM ammonium

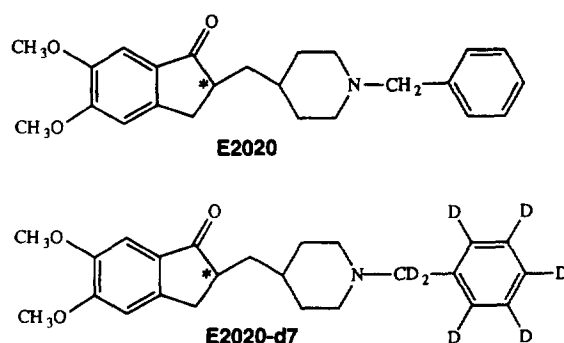


Fig. 1. Structures of E2020 and the internal standard (E2020-d<sub>7</sub>). The asterisk indicates an asymmetric carbon.

acetate (pH 7.8) at a flow-rate of 1 ml/min, and a 5- $\mu$ m Biopstick AV-1 column of 150 mm × 1.5 mm I.D. (GL Sciences) as an analytical column was eluted with 50 mM ammonium acetate (pH 5.3) containing 24% methanol and 1.5% glycerol at a flow-rate of 0.1 ml/min. There was no effect of glycerol in the mobile phase on the separation of the enantiomers except for the retention time of each enantiomer.

The MS analyses were performed with a JMS-SX102A instrument (JEOL, Tokyo, Japan) with a frit-FAB interface. MS ionization in the FAB positive-ion mode was performed with a xenon atom beam from a saddle field gun operated at 6 kV and 5 mA. The acceleration voltage, MS resolution and emission current were 10 kV, 1000 and 5 mA, respectively. The mass spectrometer was a DA700 system (Hewlett-Packard, Avondale, PA, USA) operating in the selected-ion monitoring (SIM) mode, where the target ions were at *m/z* 380 and 387 at a switching rate of 1000 ms per scan. The introduction to the frit-FAB-MS system was performed by using a pneumatic splitter [11] (Model MS-PNS; JEOL) in order to lower the flow-rate from 100 to 5  $\mu$ l/min.

### 2.3. Column-switching procedure

As shown in Fig. 2, the system consisted of two LC instruments, which were run independently. In the first stage, the plasma samples were injected directly into the trapping column,

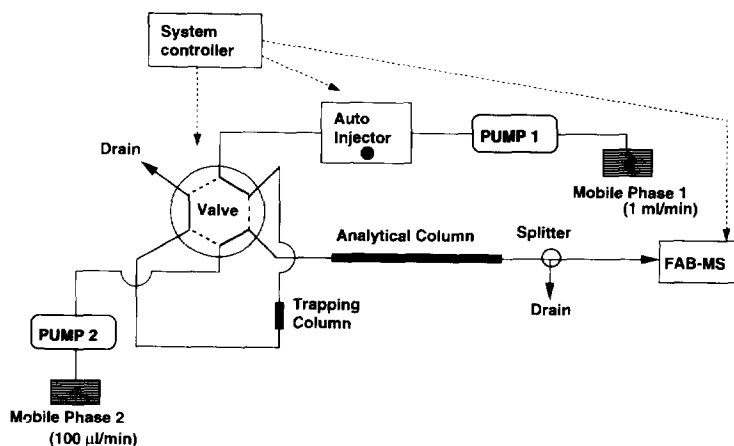


Fig. 2. Schematic diagram of the automated column-switching system for LC-MS.

plasma proteins and other hydrophilic constituents were then washed out and E2020 and E2020-d<sub>7</sub> were retained. In second stage, the valve was switched and E2020 and E2020-d<sub>7</sub> were transferred to the analytical column, where the enantiomers were optically resolved. Further, the flow from the analytical column was split and about 5% of the total flow was transferred to the frit-FAB interface, because the introduction of mobile phase into the MS ion source was restricted. After the completion of these two stages, the procedure was repeated with another sample.

#### 2.4. Preparation of standard solutions

A racemic mixture of E2020 was used as standards for each enantiomer of E2020. A stock standard solution of racemic E2020 was prepared by dissolution in 0.0001 M hydrochloric acid at a concentration of 10 µg/ml and dilution to make calibration standards. A stock standard solution of E2020-d<sub>7</sub> (racemic mixture) was prepared by dissolution in 0.0001 M hydrochloric acid at a concentration of 500 ng/ml. These solutions were stored at 4°C.

#### 2.5. Quality control sample preparation

Quality control samples were prepared by

adding an E2020 enantiomer to a pool of dog blank plasma. The plasma pool was divided into 0.5-ml aliquots and stored frozen at -20°C.

#### 2.6. Sample preparation

To 0.5 ml of the plasma sample were added 100 µl of the E2020-d<sub>7</sub> solution (500 ng/ml). The resulting mixture was vortex mixed for 1 min and centrifuged and the supernatant was transferred into a disposable syringe and filtered with a Millex-GV filter (Millipore, Tokyo, Japan), in order to remove solid particles. Then 500 µl of the filtered fluid were injected into the LC-MS system.

#### 2.7. Calculation of concentration

Peak areas of E2020 enantiomer and E2020-d<sub>7</sub> enantiomer on the selected-ion chromatograms were read by the DA700 system. Peak-area ratios ( $Q_T$ ) of the E2020 enantiomer to E2020-d<sub>7</sub> enantiomer were calculated, then the results for calibration standards were fitted to the following equation:

$$Q_T = AC_p + B$$

where  $C_p$  is the added concentration. The values of  $A$  and  $B$  were determined by non-linear least-

squares regression analysis, using a weighting factor of  $1/Y^2$ . This fitting was performed using the Multi program [12].

Measured concentrations were expressed as ng/ml of E2020 as hydrochloride (1 ng of this salt form is equivalent to 0.912 ng of free base).

### 2.8. Validation studies

The intra-assay variability was determined for five replicates of spiked samples at each calibration concentration, which were assayed against a single calibration graph.

The inter-assay variation was determined by analysis of spiked plasma samples (QC samples) on separate occasions, relative to calibration samples which were freshly prepared each time.

### 2.9. Animal samples

Male beagle dogs, obtained from CSK Research Park (Gifu, Japan), weighing about 10 kg and aged 8 months, were used. The animals were fasted from 5.00 pm on the day before dosing, with access to water ad libitum. E2020 enantiomer was administered according to a cross-over design with 1 week of a wash-out period between each administration.

The E2020 enantiomer dissolved in ethanol was intravenously administered (in about 10 s), via the cephalic vein using a disposable syringe at a dose of 1.0 mg/kg. Blood samples of 1.5 ml were drawn into heparin-treated disposable syringes, from the cephalic vein immediately before and at 5, 15 and 30 min and 1, 2, 4, 6, 8, 10, 12 and 24 h after intravenous administration of E2020. Blood was separated by centrifugation at 4°C at 3000 rpm (KL20000T centrifuge; Kubota, Tokyo, Japan) for 10 min, and 0.5 ml of plasma was then taken and stored at -20°C until analysis.

## 3. Results and discussion

### 3.1. Clean-up and chromatographic conditions

A typical chromatogram of filtered plasma sample, which was injected directly into the

avidin column (150 mm × 4.6 mm I.D.), is presented in Fig. 3. Although the enantiomeric resolution is best in the mobile phase at pH 5.3, enantiomers were eluted at pH 7 in this chromatogram because plasma proteins were retained on the column and were not eluted at pH 4–5 [4]. Plasma proteins and other hydrophilic components were not absorbed and were excluded from the avidin column within 5 min. On the other hand, E2020 enantiomers were retained on the avidin column and these enantiomers were separated.

The plausible metabolic pathways of E2020 are shown in Fig. 4. For E2020, demethylation followed by O-glucuronide conjugation, N-dealkylation, N-oxidation or aromatic hydroxylation and then sulfate conjugation were the main metabolic pathways. The chromatograms of E2020 and its six metabolites (M1–M6) are shown in Fig. 5. The avidin column separates all

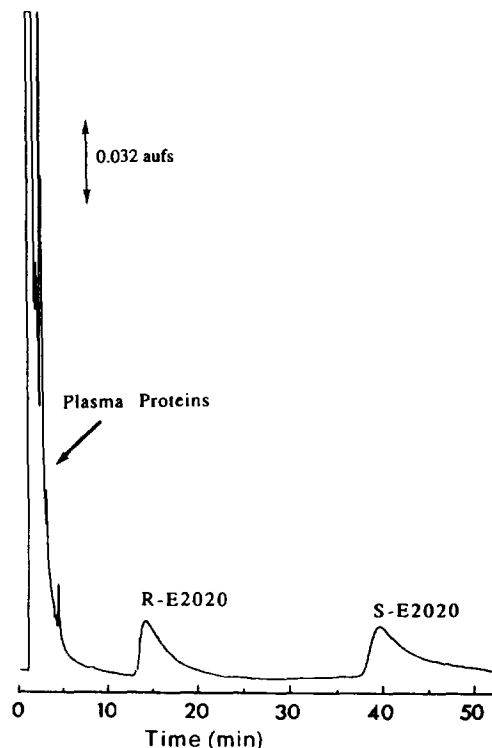


Fig. 3. Chromatogram of racemic E2020 (2 µg) in plasma after direct injection. Mobile phase, 7.5% acetonitrile in 0.1 M phosphate buffer (pH 7); flow-rate, 1.0 ml/min; detection, UV at 270 nm.

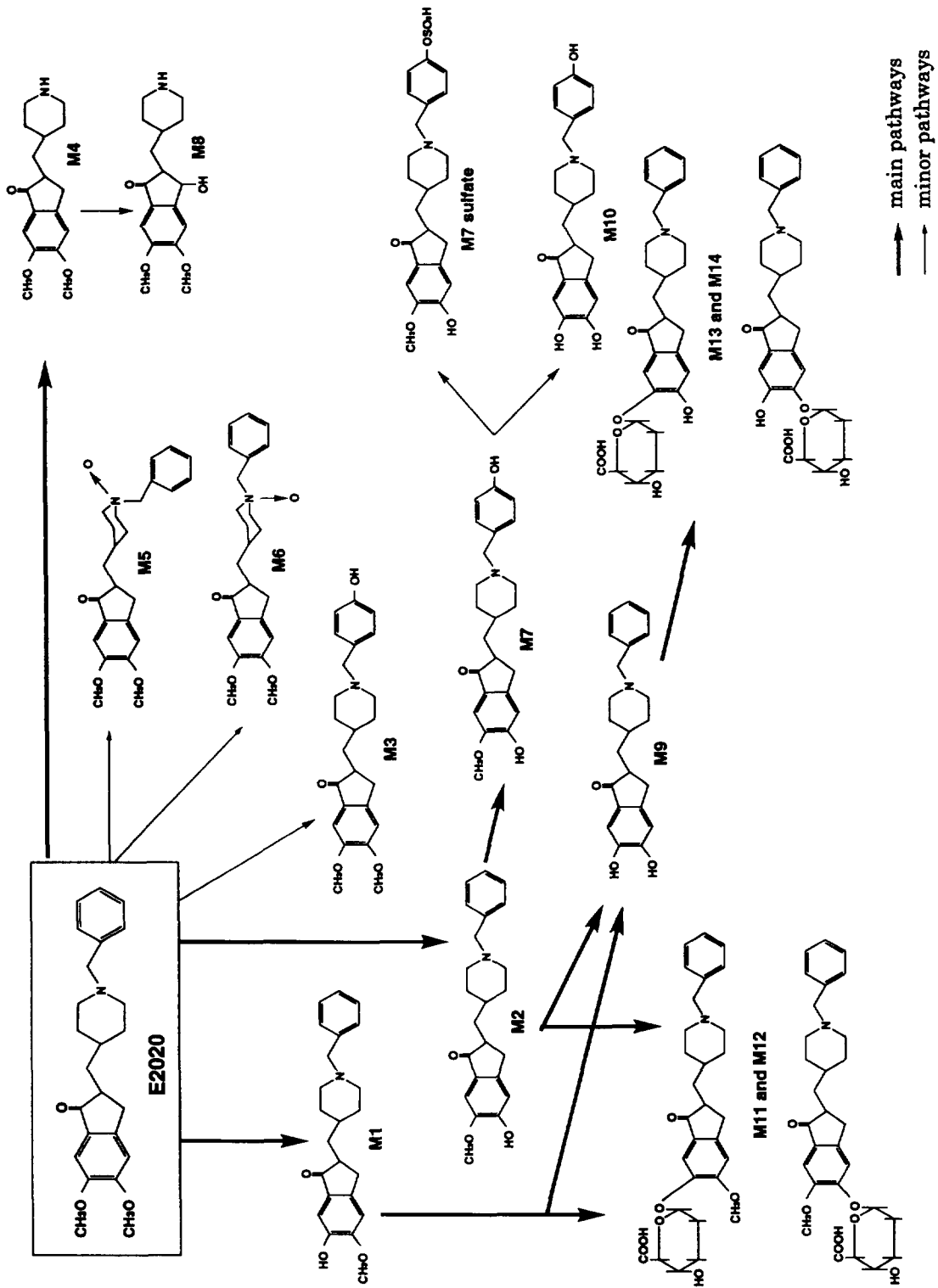


Fig. 4. Plausible metabolic pathways of E2020.

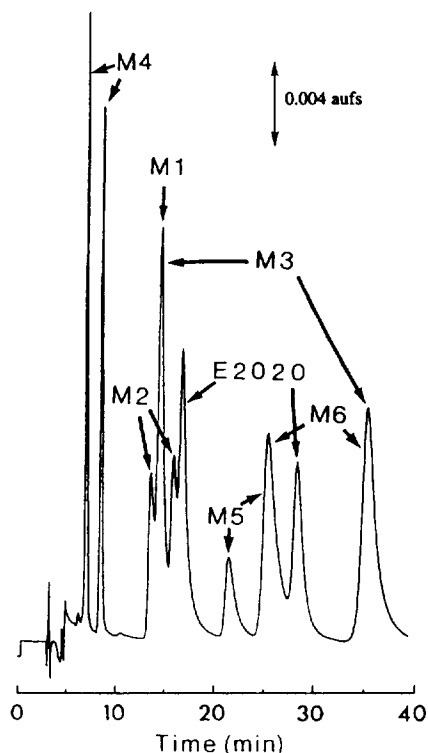


Fig. 5. Chromatogram of E2020 and its six metabolites in plasma after the column-switching procedure. Mobile phase for trapping E2020 and metabolites, 0.2 M ammonium acetate buffer (pH 5); mobile phase for enantioselective separation, 5% acetonitrile in 0.1 M phosphate buffer (pH 5); detection, UV at 271 nm.

their enantiomers except M1, so ten peaks on the chromatogram were detected. It seems to be difficult to find the optimum condition to separate E2020 enantiomers from all the metabolites. Therefore, we investigated the use of MS to detect E2020 enantiomers specifically without interference from metabolites and plasma constituents. As the introduction of the mobile phase from LC is restricted, the eluent from conventional LC columns must be split and only a small fraction of the mobile phase flow passes into the MS ion source. However, the flow from microbore columns is very low so that the use of a microbore avidin column not only gives high mass sensitivity but also improves the splitting

ratio at the interface [13]. In this study, the column-switching technique was employed using a microbore avidin column (150 mm  $\times$  1.5 mm I.D.) as analytical column. This column-switching technique has the advantages that it allows the on-line measurement of enantiomers without any clean-up procedure, high sensitivity can be achieved as the result of concentration of sample on the trapping column and enantiomers are separated effectively in the mobile phase at pH 5.3.

An internal standard method was employed to compensate for run-to-run variability in the efficiency of the frit-FAB ionization process. E2020- $d_7$  was used as the internal standard.

### 3.2. Mass spectrometric conditions

The FAB mass spectrum of E2020 is shown in Fig. 6. The major ion was the protonated molecular ions as the base peaks ( $m/z$  380) and only a few fragment ions were observed. The ion at  $m/z$  380 for E2020 was not detected in the mass spectra of E2020- $d_7$ , M1, M2, M3, M4, M5, M6, M1-glucuronide and M2-glucuronide (data not shown). Therefore, the ions at  $m/z$  380 and 387 were monitored by SIM as the target ions. Fig. 7 shows typical SIM chromatograms for blank and spiked plasma samples.

### 3.3. Limit of detection

Detection by MS and UV in this method were compared. The detection limit with MS (50 pg) was 100 times lower than that with a conventional UV detector (5 ng) (data not shown).

### 3.4. Linearity of calibration graph

Visual examination indicated that the responses of (*R*)- and (*S*)-E2020 were linear with respect to the concentration of E2020 enantiomers added. This was confirmed by the determination of the intra-assay variability (Tables 1 and 2).

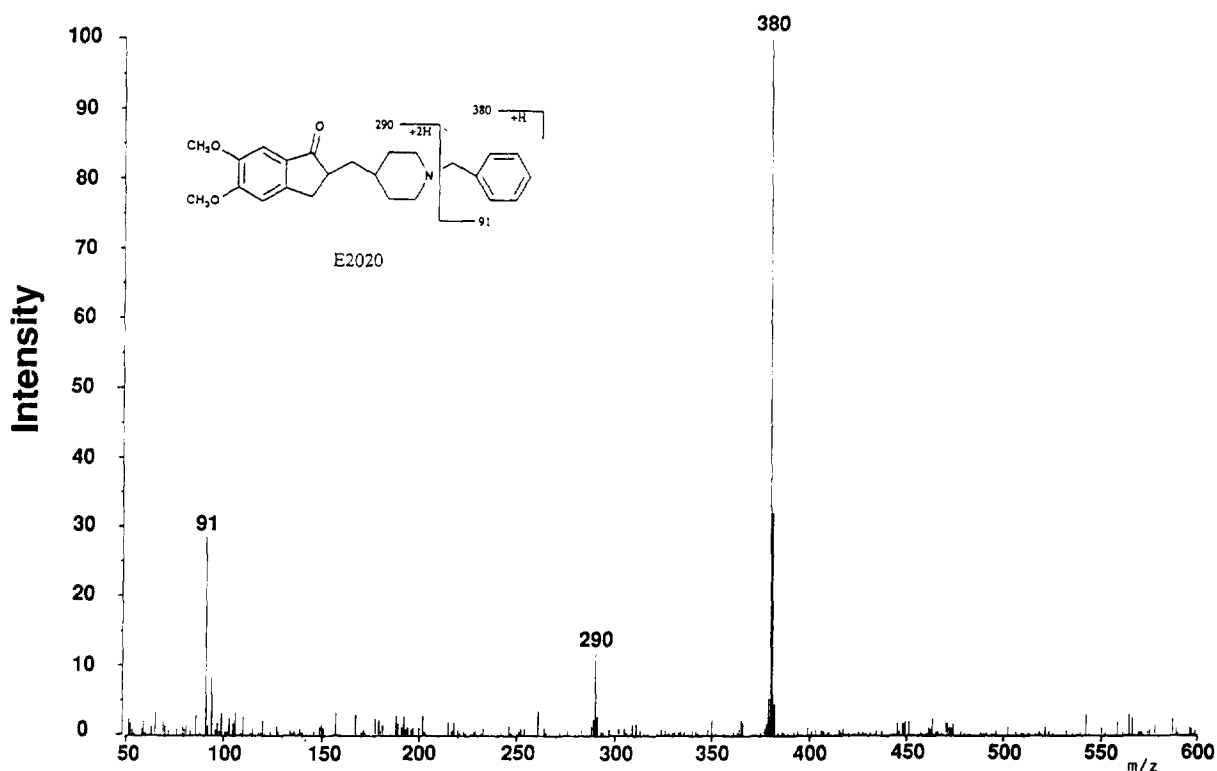


Fig. 6. Positive product ion mass spectra (background subtracted) of the protonated molecular ions of E2020; 20 ng of substance analyzed by LC-MS.

### 3.5. Assay validation

The intra- and inter-assay precision of the analysis were examined with samples of dog plasma spiked with E2020 enantiomers.

As shown in Tables 1 and 2, the intra-assay variability was determined for five replicates of spiked samples at each calibration concentration, which were assayed against a single calibration graph. The intra-assay relative standard deviations (R.S.D.s) in the range 1.00–502 ng/ml of each enantiomer were within 5.2% and the accuracy was from -7.4 to +7.6%, indicating that this method is reliable within that range.

As shown in Tables 3 and 4, the inter-assay variation was determined by analysis of the spiked plasma samples (QC samples) on three separate occasions, relative to calibration samples that were freshly prepared each time. The

inter-assay R.S.D.s in the range 1.00–502 ng/ml of each enantiomer were within 4.5% and the accuracy was from -4.8 to +4.0%, indicating that this method is reliable within that range.

These results indicate that the use of an internal standard, i.e., a stable isotope of E2020, is very effective for reproducibility of determination by LC-MS.

### 3.6. Limit of quantification

Based on the results of the assay validation, the limit of quantification was set at 1.00 ng/ml.

### 3.7. Plasma samples

The method was applied to the simultaneous determination of the enantiomers of E2020 in

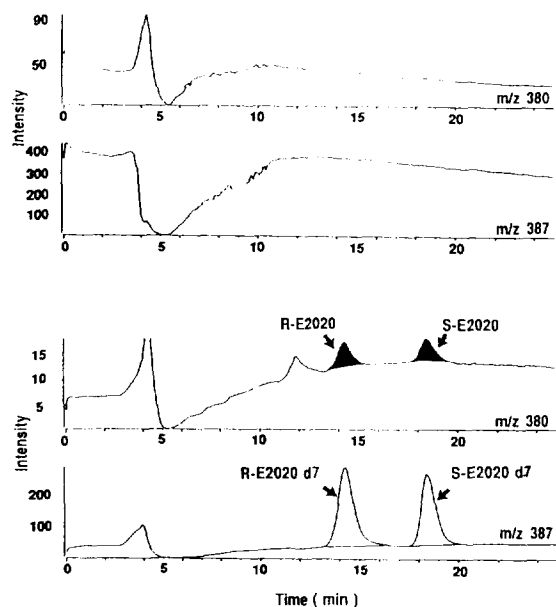


Fig. 7. Typical selected-ion chromatograms of the enantioselective separation of the enantiomers of E2020 and E2020-d<sub>7</sub>. (Top) blank plasma; (bottom) plasma sample spiked with 0.5 ng of E2020 and 50 ng of E2020-d<sub>7</sub>.

dog plasma undergoing treatment with (*R*)- or (*S*)-E2020.

The mean plasma levels of (*R*)-E2020 at 5 min after intravenous administration of (*R*)-E2020 (optical purity 99.43%), the first time point of sampling, was 290 ng/ml. This was followed by a biphasic exponential decline, with an apparent

$t_{1/2}$  for the terminal phase of  $3.05 \pm 0.71$  h. Similarly, the mean plasma levels of (*S*)-E2020 (optical purity 98.25%) was 400 ng/ml and then showed biphasic exponential decline, with an apparent  $t_{1/2}$  for the terminal phase of  $2.87 \pm 0.27$  h. These results indicated that there is no difference in the pharmacokinetic profiles of (*R*)- and (*S*)-E2020 in dogs.

Moreover, the concentration of (*S*)-E2020 5 min after intravenous administration of (*R*)-E2020 and of (*R*)-E2020 5 min after intravenous administration of (*S*)-E2020 corresponded to the concentration of optical impurity in the dosing solution, and the mean plasma levels of (*S*)-E2020 after intravenous administration of (*R*)-E2020 showed a biphasic exponential decline with an apparent  $t_{1/2}$  for the terminal phase of  $2.73 \pm 0.52$  h, which is very similar to the  $t_{1/2}$  of (*R*)-E2020 after administration of (*R*)-E2020. These results indicate that, even if E2020 enantiomers interconvert in plasma, the interconversion is very slow after intravenous administration to dogs.

#### 4. Conclusions

The LC-MS method using column-switching techniques described in this paper is sensitive, reproducible, precise and stable. The method was found to be applicable to the study of the

Table 1  
Intra-assay validation for (*R*)-E2020 in plasma ( $n = 5$ )

Parameter	Theoretical concentration (ng/ml)								
	1.00	2.51	5.02	10.0	25.1	50.2	100	251	502
Measured concentration (ng/ml)	1.02	2.40	4.62	9.72	24.9	49.0	102	270	512
	1.03	2.35	4.61	9.67	25.5	50.6	103	268	517
	0.97	2.33	4.28	9.93	25.7	49.9	102	271	510
	0.94	2.43	4.81	9.71	26.0	50.0	109	266	512
	0.97	2.32	4.92	9.72	25.1	51.1	103	275	513
Mean	0.99	2.37	4.65	9.75	25.4	50.1	104	270	513
S.D.	0.04	0.05	0.24	0.1	0.44	0.79	2.95	3.39	2.59
R.S.D. (%)	4.0	2.1	5.2	1.0	1.7	1.6	2.8	1.3	0.5
Accuracy (%)	-1.0	-5.6	-7.4	-2.5	1.2	-0.2	4.0	7.6	2.2



Table 2  
Intra-assay validation for (*S*)-E2020 in plasma ( $n = 5$ )

Parameter	Theoretical concentration (ng/ml)								
	1.00	2.51	5.02	10.0	25.1	50.2	100	251	502
Measured concentration (ng/ml)	1.06	2.37	4.82	9.84	26.4	48.9	104	267	499
	1.03	2.55	5.05	9.54	26.1	49.8	104	258	499
	1.04	2.42	4.69	9.21	25.9	50.4	102	256	520
	1.02	2.43	4.62	9.75	26.9	48.0	100	263	506
	0.98	2.42	4.61	9.40	25.6	50.4	102	256	524
Mean	1.03	2.44	4.76	9.55	26.2	49.5	102	260	510
S.D.	0.03	0.07	0.18	0.26	0.5	1.04	1.67	4.85	11.76
R.S.D. (%)	2.9	2.9	3.8	2.7	1.9	2.1	1.6	1.9	2.3
Accuracy (%)	3.0	-2.8	-5.2	-4.5	4.4	-1.4	2.0	3.6	1.6

Table 3  
Intra-assay validation for (*R*)-E2020 in plasma ( $n = 3$ )

Parameter	Theoretical concentration (ng/ml)								
	1.00	2.51	5.02	10.0	25.1	50.2	100	251	502
Measured concentration (ng/ml)	0.97	2.44	4.90	9.83	25.1	49.5	97.7	242	483
	1.03	2.49	5.11	10.6	25.3	51.0	101	251	510
	0.95	2.56	4.70	9.82	24.3	48.0	98.1	255	508
Mean	0.98	2.50	4.90	10.1	24.9	49.5	98.9	249	500
S.D.	0.04	0.06	0.21	0.45	0.53	1.50	1.80	6.66	15.04
R.S.D. (%)	4.1	2.4	4.3	4.5	2.1	3.0	1.8	2.7	3.0
Accuracy (%)	-2.0	-0.4	-2.4	1.0	-0.8	-1.4	-1.1	-0.8	-0.4

Table 4  
Intra-assay validation for (*S*)-E2020 in plasma ( $n = 3$ )

Parameter	Theoretical concentration (ng/ml)								
	1.00	2.51	5.02	10.0	25.1	50.2	100	251	502
Measured concentration (ng/ml)	1.00	2.37	4.92	10.4	25.5	50.0	99.0	251	501
	0.98	2.41	4.88	10.0	25.1	51.8	105	255	499
	1.00	2.39	4.98	10.0	25.5	50.3	108	257	507
Mean	0.99	2.39	4.93	10.1	25.5	50.3	104.0	254	502
S.D.	0.01	0.02	0.05	0.23	0.4	1.42	4.58	3.06	4.16
R.S.D. (%)	1.0	0.8	1.0	2.3	1.6	2.8	4.4	1.2	0.8
Accuracy (%)	-1.0	-4.8	-1.8	1.0	1.6	0.2	4.0	1.2	0.0

pharmacokinetics of E2020 in biological samples and is the first reported assay capable of measuring the enantiomeric concentration of E2020 in plasma.

## References

- [1] Y. Yamanishi, *Basic, Clinical, and Therapeutic Aspect of Alzheimer's and Parkinson's Diseases*, Vol. 2, Plenum Press, New York, 1990, p. 409.
- [2] E.J. Ariens, *Eur. J. Clin. Pharmacol.*, 26 (1974) 663.
- [3] J. van der Grief, W.M.A. Niessen and U.R. Tjaden, *J. Chromatogr.*, 474 (1989) 5.
- [4] P. Kokkonen, W.M.A. Niessen, U.R. Tjaden and J. van der Grief, *J. Chromatogr.*, 474 (1989) 59.
- [5] A. Walhagen, L.E. Edholm, C.E.M. Heeremans, R.A.M. van der Hoeven, W.M.A. Niessen, U.R. Tjaden and J. van der Grief, *J. Chromatogr.*, 474 (1989) 257.
- [6] W. Luiten, G. Damien and J. Capart, *J. Chromatogr.*, 474 (1989) 265.
- [7] E.R. Verheij, H.J.E.M. Reeuwijk, W.M.A. Niessen, U.R. Tjaden, J. van der Grief and G.F. LaVos, *Biomed. Environ. Mass Spectrom.*, 16 (1989) 393.
- [8] Y. Oda, N. Asakawa, S. Abe, Y. Yoshida and T. Sato, *J. Chromatogr.*, 572 (1991) 133.
- [9] Y. Oda, H. Ohe, N. Asakawa, Y. Yoshida, T. Sato, and T. Nakagawa, *J. Liq. Chromatogr.*, 15 (1992) 2997.
- [10] N. Asakawa, H. Ohe, M. Tsuno, Y. Yoshida and T. Sato, *J. Chromatogr.*, 541 (1991) 231.
- [11] T. Kobayashi, presented at the 36th ASMS Conference on Mass Spectrometry and Allied Topics, 5–10 June, 1988, San Francisco, CA.
- [12] K. Yamaoka, *J. Pharmacobio-Dyn.*, 4 (1981) 879.
- [13] Y. Oda, N. Asakawa, Y. Yoshida and T. Sato, *J. Pharm. Biomed. Anal.*, in press.